

Conductance and Kondo Interference beyond Proportional Coupling

Luis G. G. V. Dias da Silva,¹ Caio H. Lewenkopf,² Edson Vernek,³ Gerson J. Ferreira,³ and Sergio E. Ulloa⁴

¹*Instituto de Física, Universidade de São Paulo, C.P. 66318, 05315-970 São Paulo, São Paulo, Brazil*

²*Instituto de Física, Universidade Federal Fluminense, 24210-346 Niterói, Brazil*

³*Instituto de Física, Universidade Federal de Uberlândia, Uberlândia, Minas Gerais 38400-902, Brazil.*

⁴*Department of Physics and Astronomy, and Nanoscale and Quantum Phenomena Institute, Ohio University, Athens, Ohio 45701-2979, USA*

(Received 27 February 2017; published 12 September 2017)

The transport properties of nanostructured systems are deeply affected by the geometry of the effective connections to metallic leads. In this work we derive a conductance expression for a class of interacting systems whose connectivity geometries do not meet the Meir-Wingreen proportional coupling condition. As an interesting application, we consider a quantum dot connected coherently to tunable electronic cavity modes. The structure is shown to exhibit a well-defined Kondo effect over a wide range of coupling strengths between the two subsystems. In agreement with recent experimental results, the calculated conductance curves exhibit strong modulations and asymmetric behavior as different cavity modes are swept through the Fermi level. These conductance modulations occur, however, while maintaining robust Kondo singlet correlations of the dot with the electronic reservoir, a direct consequence of the lopsided nature of the device.

DOI: [10.1103/PhysRevLett.119.116801](https://doi.org/10.1103/PhysRevLett.119.116801)

The quantum coupling of spatially localized discrete levels to cavity modes has emerged as a key tool for quantum information processing in different contexts, from cavity systems in atoms [1] and semiconductor quantum dots [2] to exciton-polariton condensates in optical systems [3]. Similarly, coherent coupling of electronic modes to discrete quantum systems has been explored in quantum corrals created on metallic surfaces [4], allowing the manipulation and control of quantum information over regions a few nanometers across [5]. Recent experiments have extended this fascinating line of inquiry to systems implemented on two-dimensional electronic structures in semiconductors [6,7]. These new systems have paved the way for quantum engineering in integrated, scalable nanoscale systems with great flexibility on geometries and interesting physical behavior.

The control of quantum dot (QD) characteristics in these systems, such as the tunnel coupling to external current leads, have also allowed the experimental study of the Kondo regime, an emblematic many-body effect [8,9]. In this regime, the net magnetic moment of an unpaired spin in the QD becomes effectively screened by the conduction electrons in the leads, forming a delocalized quantum singlet that involves correlations with the electronic spins in the lead reservoirs [10]. Moreover, the coupling of a QD to reservoirs with nontrivial energy dependence gives rise to a variety of interesting effects on the ensuing Kondo state, including the appearance of zero-field splittings of the Kondo resonance [11–13]. As QD systems are designed to interact with increasingly complex structures, one is led to ask how such many-body correlations would evolve.

The standard theoretical tool for the description of the two-terminal conductance through interacting regions is the

Meir-Wingreen (MW) generalization of the Landauer formula for correlated systems [14]. The MW expression is particularly useful in cases where the coupling matrix elements between the leads and the system are related to each other by a multiplicative factor. This condition was later dubbed “proportional coupling” (PC) [15] and it is essential in writing the conductance in terms of the system’s retarded Green’s function. In many cases, however, the PC description is inadequate [16] and the evaluation of the conductance requires an alternative treatment.

A remarkable example of a nanoscale device with non-PC geometry was recently investigated in Ref. [6]. They demonstrated coherent coupling between a QD in the Coulomb blockade regime and a larger, cavitylike region inscribed electrostatically onto the same two-dimensional electron gas (2DEG). The QD is coupled to two metallic leads while the cavity itself is coupled to only one of them, clearly breaking the PC condition. The size of the cavity and its coupling to the QD can be controlled by gate voltages on the device, allowing for fine control over the spacing between cavity resonances, the tunnel rate of electrons between cavity and the QD, and the dot-cavity coupling over a wide range, while studying the conductance of the entire structure.

In this Letter we extend the applicability of the MW expression to a large class of non-PC cases, providing theoretical tools to analyze the transport properties and temperature dependence of systems with a single interacting level (such as a QD) embedded in complex structures, as some studied recently [6,7]. We find it is possible to write the linear conductance of such systems as

$$G = \frac{2e^2}{\hbar} \frac{\tilde{\Gamma}_L(\epsilon_F)\tilde{\Gamma}_R(\epsilon_F)}{\tilde{\Gamma}_L(\epsilon_F) + \tilde{\Gamma}_R(\epsilon_F)} \int d\omega \left(-\frac{\partial f_0}{\partial \omega} \right) A_d(\omega), \quad (1)$$

where f_0 is the equilibrium Fermi function, the couplings $\tilde{\Gamma}_{L,R}(\epsilon_F)$ are effective hybridization functions to left (L) and right (R) leads, $A_d(\omega) = (-1/\pi)\text{Im}G_d^r(\omega)$ the spectral function, and G_d^r is the retarded Green's function at the QD.

The latter two functions can be accurately calculated through a variety of techniques, such as Wilson's numerical renormalization group (NRG) [17].

Although deceptively similar to the MW conductance formula for a single-level QD [15], this expression incorporates the connection of the entire complex system to each lead through the effective hybridization functions $\tilde{\Gamma}_{L,R}(\epsilon_F)$. A crucial difference is that, in the original formula [14], the hybridization is represented by matrices of functions $\Gamma^{L,R}$ involving the couplings and the density of states in the leads. Here, such complexities are encoded in the intricate energy structure of $\tilde{\Gamma}_{L,R}(\omega)$. As we will see below, these functions can be obtained after careful consideration of the effective connectivity of the system.

Next, we use this approach to successfully describe and provide further insight on conductance measurements of a QD coupled to a cavity [6]. We implement a realistic model of the curved electrostatic reflector used to define the cavity in experiments, utilizing both analytical and numerical approaches. We further calculate the QD spectral density required by Eq. (1) by applying the NRG to an effective Anderson model that incorporates the cavity. Our results show contrasting transport properties in the weak- and strong-coupling regimes, in excellent agreement with experiments. As the coupling to the cavity sets in, the conductance is strongly modulated, especially as different cavity resonances are swept through the Fermi level in the leads by applied gates [6]. Moreover, the NRG calculations allow us to relate the conductance behavior to other intrinsic characteristics, such as the Kondo temperature T_K . We find that even as the conductance peaks are strongly distorted due to the interaction with the cavity modes, the Kondo screening remains robust, with larger T_K values for stronger cavity coupling.

MW formula beyond proportional coupling.—Proportional coupled systems are those in which the coupling matrices of the interacting system to L and R leads are proportional to each other, namely, $\Gamma^R(\omega) = \lambda\Gamma^L(\omega)$ where λ is a constant factor [14]. This condition is clearly violated in the case of a QD connected to a cavity on only one lead, such as in Fig. 1. An electron in the dot is transmitted from L by a direct tunneling process regulated by the coupling matrix element V_{dL} and the density of states in that lead. In contrast, the transmission to the right involves the coherent interference between multiple paths that include the cavity resonances and states in R . Figure 1(b)

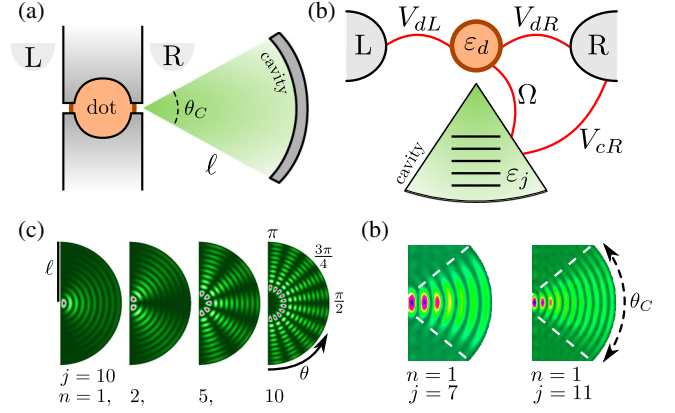


FIG. 1. (a) Experimental dot + cavity system; the cavity has radius ℓ and aperture θ_C . (b) Schematic of single-level dot (ϵ_d) coupled to multimode cavity (ϵ_j). The dot is connected to leads (L and R), while the cavity is only coupled to the R lead; coupling matrix elements are indicated. (c) Cavity modes for $\theta_C = \pi$ are described by Bessel modes $\psi_{n,j}(r, \theta)$. The $n = 1$ modes dominate the LDOS at $r \approx 0$. (d) Kwant mode simulation for finite aperture cavity ($\theta_C = \pi/2$) coupled to wide leads shows good agreement with Bessel modes.

indicates the different dot-lead (V_{dR}), and cavity-lead (V_{cR}) couplings that enter as nonzero elements in Γ^R , while the cavity-lead couplings are zero in Γ^L , thereby making the system evidently nonproportional [18].

The main technical difficulty in obtaining a transport formula is the calculation of the lesser Green's functions matrix $\mathbf{G}^<$ for the interacting region, which appears in the general expression for the current [14]. The latter gives the current through the L (R) lead as

$$J_{L(R)} = \frac{ie}{\hbar} \int d\omega \text{tr}(\Gamma^{L(R)}(\omega) \{ \mathbf{G}^<(\omega) + f_{L(R)}(\omega) [\mathbf{G}^r(\omega) - \mathbf{G}^a(\omega)] \}), \quad (2)$$

where $\mathbf{G}^{r(a)}$ is the retarded (advanced) Green's function matrix [18] and $f_{L(R)}$ is the Fermi distribution at the L (R) lead with chemical potential $\mu_{L(R)}$. Proportional coupling and current conservation make it possible to simplify the calculation by ingeniously writing $J_{L(R)}$ in terms of $\mathbf{G}^{r(a)}(\omega)$. In contrast, for interacting non-PC systems away from equilibrium, the elimination of $\mathbf{G}^<$ is in general not possible. However, in the linear response regime it can be achieved by recalling that [16]

$$\mathbf{G}^<(\omega) \approx \mathbf{G}_{\text{eq}}^<(\omega) - \frac{\partial f_0}{\partial \omega} \Pi(\omega) \Delta\mu + O(\Delta\mu^2), \quad (3)$$

where $\Delta\mu = \mu_L - \mu_R$ and $\Pi(\omega)$ has a slow ω dependence within energy windows of $k_B T$ corresponding to the experiments of interest. These conditions eventually lead to Eq. (1); the detailed derivation is provided in the

Supplemental Material [18]. Notice that the structure of the system may result in a cumbersome derivation of the $\tilde{\Gamma}_{L,R}(\omega)$ entering Eq. (1). We now specify the QD-cavity model that exemplifies this treatment.

Resonant cavity modes.—The key experimental element is a “mirror” that focuses resonant modes onto the QD, both elements electrostatically defined on a 2DEG. The cavity has a length $\ell \sim 2 \mu\text{m}$ and angular aperture $\theta_C \sim 45^\circ$, as indicated in Fig. 1(a). Assuming circular symmetry, the normal modes are given by Bessel functions, $\psi_{n,j}(r, \theta) \approx J_n(k_{n,j}r) \sin(n\theta)$. The dot-cavity coupling is maximal for modes with the largest amplitude in the vicinity of $r \approx 0$, and dominated by resonances with $n = 1$, given that $J_n(kr) \propto (kr)^n$ for $kr \ll 1$. These modes have a characteristic energy spacing $\delta_{\text{cav}} \approx 200 \mu\text{eV}$ for a cavity with these dimensions, in agreement with the resonance separations in the experiment [6] and confirmed by Kwant calculations [18,25].

It is remarkable that although the cavity is immersed in the R lead, it can be tuned to produce sharply peaked resonances that strongly modify $\tilde{\Gamma}_R(\omega)$, providing different electronic paths for the current. In the experiment, a gate voltage shifts the cavity resonance levels and the coupling to the QD. This tunability can be incorporated in the interacting QD model as follows.

Interacting quantum impurity model.—The Hamiltonian for this system can be written as $H = H_{\text{dot}} + H_{\text{cavity}} + H_{\text{leads}} + H_{\text{coupling}}$, where

$$H_{\text{dot}} = \sum_{\sigma} \varepsilon_d c_{d\sigma}^{\dagger} c_{d\sigma} + U n_{d\uparrow} n_{d\downarrow}, \quad (4)$$

$$H_{\text{cavity}} = \sum_{j,\sigma} \varepsilon_j a_{j\sigma}^{\dagger} a_{j\sigma}, \quad (5)$$

$$H_{\text{leads}} = \sum_{\alpha,\mathbf{k},\sigma} \varepsilon_{\alpha\mathbf{k}} c_{\alpha\mathbf{k}\sigma}^{\dagger} c_{\alpha\mathbf{k}\sigma}. \quad (6)$$

Here $c_{d\sigma}^{\dagger}$, $a_{j\sigma}^{\dagger}$, and $c_{\alpha\mathbf{k}\sigma}^{\dagger}$ create a spin- σ electron in the dot, the j th mode of the cavity, and each of the leads $\alpha = L, R$. The resonances are assumed equally spaced, $\varepsilon_j = \varepsilon_c + (j-1)\delta_{\text{cav}}$, where ε_c is shifted by a gate voltage; leads have a flat density of states $\rho(\omega) = \rho_0 \Theta(D - |\omega|)$, symmetric about the Fermi energy ($\omega = 0$). For simplicity all couplings are assumed local, real, and independent of either momentum in the leads or cavity-mode index j . The coupling Hamiltonian is then, see Fig. 1(b),

$$H_{\text{coupling}} = \sum_{\alpha,\mathbf{k},\sigma} V_{d\alpha} c_{d\sigma}^{\dagger} c_{\alpha\mathbf{k}\sigma} + V_{cR} \sum_{j,\mathbf{k},\sigma} a_{j\sigma}^{\dagger} c_{R\mathbf{k}\sigma} + \Omega \sum_{j,\sigma} c_{d\sigma}^{\dagger} a_{j\sigma} + \text{H.c.} \quad (7)$$

QD effective decay widths.—As the Coulomb interactions are localized in the QD, one can find its effective couplings to L and R leads and the cavity, by calculating the dot retarded Green’s function for the system with $U = 0$,

$G_d^{(0),r}(\omega^+) \equiv \langle\langle c_{d\sigma}; c_{d\sigma}^{\dagger} \rangle\rangle_{\omega}$. In the wideband limit for the leads, $\sum_{\mathbf{k}} (\omega^+ - \varepsilon_{\mathbf{k}})^{-1} \rightarrow -i\pi\rho_0$, we obtain $G_d^{(0),r}(\omega) = [\omega - \varepsilon_d - \Sigma_d^{(0)}(\omega)]^{-1}$, where

$$\Sigma_d^{(0)}(\omega) = -\frac{i}{2}(\Gamma_{dL} + \Gamma_{dR}) + \left(\Omega - \frac{i}{2} \sqrt{\Gamma_{dR}\Gamma_{cR}} \right)^2 \tilde{S}(\omega), \quad (8)$$

is the noninteracting self-energy. Here, $\Gamma_{(c,d)\alpha} \equiv 2\pi\rho_0 |V_{(c,d)\alpha}|^2$, for $\alpha = L, R$, with the cavity structure contained in $S(\omega) \equiv \sum_j (\omega - \varepsilon_j)^{-1}$ and $\tilde{S}(\omega) = S(\omega)(1 + iS(\omega)\Gamma_{cR}/2)^{-1}$. The hybridization function of the (noninteracting) dot with the effective fermionic system is given by $\Delta(\omega) = -\text{Im}\Sigma_d^{(0)}(\omega)$. This approach can be extended to the interacting Green’s function [12,13], as long as the interactions are restricted to the QD.

The interference of cavity modes and states in the leads is contained in the structure of $\Delta(\omega)$, which yields a highly structured density of states of the “effective” Fermi reservoir in which the QD is embedded [18]. Most importantly, the structure in $\Delta(\omega)$ affects strongly the Kondo state in the system once interactions set in. $\Delta(\omega)$ reliably describes the experimental system once cavity parameters are extracted either from a microscopic model, and/or determined from experiments [26].

Conductance for the interacting system.—Equation (1) determines the conductance through the system under different cavity + QD coupling regimes. The QD coupling to the left (source) reservoir is simply $\tilde{\Gamma}_L = \Gamma_{dL}$. In contrast, the coupling to the right (drain) reservoir requires the full Green’s function and results in [18]

$$\tilde{\Gamma}_R(\omega) = \Gamma_{dR} + \Gamma_{cR} |\tilde{S}(\omega)|^2 \left(\Omega^2 + \frac{\Gamma_{cR}\Gamma_{dR}}{4} \right) + \sqrt{\Gamma_{dR}\Gamma_{cR}} \tilde{S}(\omega) \left(\Omega - \frac{i}{2} \sqrt{\Gamma_{cR}\Gamma_{dR}} \right) + \text{H.c.} \quad (9)$$

This expression encodes information about all nontrivial interference processes taking place during transport. The energy dependence of $\tilde{\Gamma}_R(\omega)$ prevents the use of the PC simplification, demanding the more general approach we put forward here. The spectral function needed in Eq. (1) is obtained by an NRG approach that uses the full intricate structure of the effective hybridization function $\Delta(\omega)$ coupling the interacting QD to the environment.

Before discussing the conductance, we analyze the QD spectral function. In general, $A_d(\omega)$ shows a sequence of asymmetric features whenever ε_c shifts cavity modes near the Fermi level ($\omega = 0$), with characteristic shape and width that changes strongly with coupling Ω . Figure 2 illustrates this behavior for weak ($\Omega < \Gamma_{cR}/2$) and strong ($\Omega > \Gamma_{cR}/2$) dot-cavity coupling regimes. For weak coupling [Fig. 2(a)&(c)], the modulation is marked by diagonal

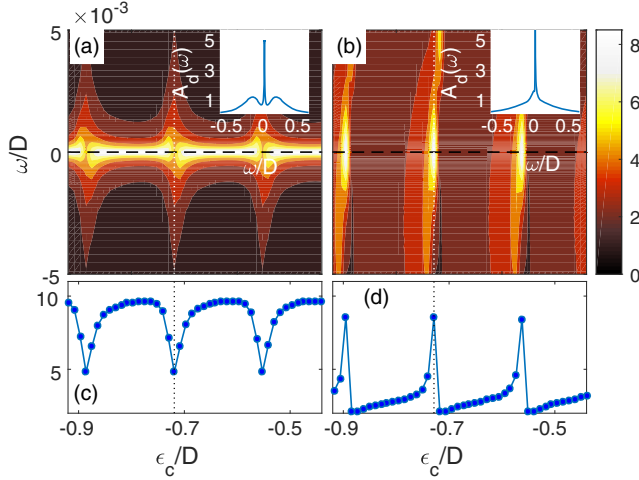


FIG. 2. NRG-calculated dot spectral density $A_d(\omega)$ for cavity gate voltages ϵ_c in the weak [$\Omega = 0.01D$, (a),(c)] and strong coupling [$\Omega = 0.15D$, (b),(d)] regimes. Panels (c) and (d) show $A_d(0)$ vs ϵ_c (cuts through the horizontal dashed lines). Peaks in $A_d(0)$ correspond to dips in $\Delta(0)$ and vice versa [18]. Insets show typical Kondo peaks in $A_d(\omega)$, present even when cavity modes dominate $\Delta(0)$ (vertical dotted lines).

“valleys” whenever a cavity mode contributes to $\Delta(0)$, separated by bright peaks in A_d . The large Ω regime [Figs. 2(b) and 2(d)] is drastically different: $\Delta(0)$ exhibits Fano asymmetric line shapes as a function of ϵ_c , leading to sharp asymmetric peaks in $A_d(\omega < T_K)$ [18].

This behavior can be qualitatively understood in terms of the Friedel sum rule (FSR) [12,27,28], as $A_d(0)$ is inversely proportional to $\Delta(0)$. Accordingly, when a resonant peak of $\Delta(\omega)$ lies close to the Fermi energy, it causes a downturn in the spectral function, and a consequent *splitting* of the Kondo peak may appear in A_d in the $\omega < T_K$ range [12]. Such splittings do appear for some ϵ_c values, where A_d shows two local maxima away from the $\omega = 0$ mark in Fig. 2(b) (see details in Ref. [18]). Nonetheless, even at these points, $A_d(\omega)$ shows fully developed Kondo resonances of width $\sim T_K$ in between Hubbard peaks [insets in Figs. 2(a) and 2(b)].

The resulting conductance G (in units of $G_0 = 2e^2/h$) is shown in Fig. 3 vs cavity voltage ϵ_c , for Ω values from $0.01D$ (weak) to $0.2D$ (strong coupling) and for $T = 0$ and 250 mK.

At low temperatures and small Ω , the conductance exhibits a quantized peak whenever a cavity resonance is near the Fermi level, in agreement with the experimental result [6]. The conductance drops away with ϵ_c as destructive interference sets in and results in a nonzero scattering shift associated with the strongly asymmetric $A_d(\omega)$, as expected from the FSR.

Conversely, when a cavity resonance is aligned with the Fermi level in the strong coupling regime, a Fano-like *dip* appears in the conductance, with a width much smaller than the cavity level spacing. This feature is also consistent with

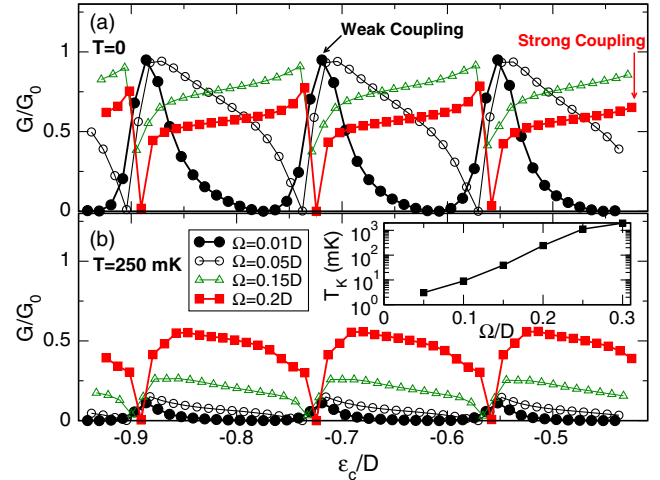


FIG. 3. Conductance G/G_0 vs cavity gate voltages ϵ_c with cavity-dot couplings ranging from the weak ($\Omega = 0.01D$) to the strong coupling regime ($\Omega = 0.2D$) for (a) $T = 0$ and (b) $T = 0.031U$ (or $T = 250$ mK for $U = 0.7$ meV). Inset: Kondo temperature as a function of cavity-dot coupling Ω for $\epsilon_c = -0.9D$.

the experimental data of Ref. [6]. Finite temperatures do not result in qualitative changes of this picture, but suppress the magnitude of G , as one would expect, with a larger effect for T_K values below the temperature of the reservoir (here 250 mK).

Notice that the spinful QD remains in the Kondo regime over this range of coupling to the cavity. In fact, the Kondo screening is stronger for larger Ω , as monitored by the value of T_K . To quantify this, we calculate T_K from the magnetic susceptibility curves obtained from the NRG, a procedure that focuses on how the Kondo fixed point is reached at lower energies, and does not rely on the behavior of the spectral density [17]. The inset in Fig. 3 shows T_K increasing rapidly with larger QD-cavity coupling Ω . For $\Omega = 0.15D - 0.2D$, we obtain $T_K \sim 0.0048U - 0.03U$; with the experimental $U = 0.7$ meV, this translates into $T_K \sim 40 - 240$ mK, which is consistent with the observed value of ~ 100 mK, obtained from the conductance peak width (see supplement in Ref. [6]). Our calculations also show T_K to depend weakly on ϵ_c . This might appear counterintuitive, as $\Delta(0)$ is strongly modulated by changes in ϵ_c , but the explanation is simple: The effective coupling defining the Kondo temperature (e.g., Γ in Haldane’s expression [29]) is given not by $\Delta(0)$, but rather by an integral over the full bandwidth, $\Gamma \propto \int \Delta(\omega) d(\omega/D)$ [30]. This “ Γ ” depends strongly on the dot-cavity coupling Ω (thereby giving the strong variation of T_K with Ω) while only weakly with ϵ_c , whose main effect is to shift the peaks in $\Delta(\omega)$.

The increasing T_K indicates that the screening of the QD spin by the composite cavity-lead environment is in fact more robust for larger Ω , which is confirmed by an NRG analysis of the thermal properties of the QD. This is

remarkable behavior, as the strong variation in $A_d(\omega)$ and resulting conductance are drastically different from the simply-connected QD in the Kondo regime.

Discussion.—We have presented an approach that allows one to calculate the linear conductance through interacting systems beyond the proportional coupling approximation. This opens the possibility of studying interesting systems with complex geometries where quantum interference introduces nontrivial energy dependence on the effective decay widths $\tilde{\Gamma}_\alpha$. We have illustrated the power of the method by analyzing a recent experiment with very interesting geometry [6]. Despite the observed splitting and strong modulation of conductance peaks for growing cavity coupling, we find that the Kondo screening is in fact strengthened, as characterized by a larger T_K . This interpretation is supported by calculations of the conductance in excellent agreement with experiment. It would be interesting to be able to measure the expected phase shifts introduced by the interaction with the cavity to provide further insights into the coherent interference that these many-body coupled systems experience.

We acknowledge useful discussions with C. Rössler, T. Ihn, K. Ensslin, and N. Sandler. L. D. S. acknowledges support from CNPq Grants No. 307107/2013-2 and No. 449148/2014-9, PRP-USP NAP-QNano and FAPESP Grant No. 2016/18495-4. S. E. U. received support from NSF Grant No. DMR 1508325, and the Aspen Center for Physics, NSF Grant No. PHY-1066293. C. H. L. is supported by CNPq Grant No. 308801/2015-6 and FAPERJ Grant No. E-26/202.917/2015. G. J. F. and E. V. acknowledge financial support from CNPq and FAPEMIG. Pro-Reitoria de Pesquisa, Universidade de São Paulo

-
- [1] J. M. Raimond, M. Brune, and S. Haroche, *Rev. Mod. Phys.* **73**, 565 (2001).
- [2] K. Hennessy, A. Badolato, M. Winger, D. Gerace, M. Atature, S. Gulde, S. Falt, E. L. Hu, and A. Imamoglu, *Nature (London)* **445**, 896 (2007).
- [3] J. Kasprzak, M. Richard, S. Kundermann, A. Baas, P. Jeambrun, J. M. J. Keeling, F. M. Marchetti, M. H. Szymanska, R. Andre, J. L. Staehli, V. Savona, P. B. Littlewood, B. Deveaud, and L. S. Dang, *Nature (London)* **443**, 409 (2006).
- [4] E. J. Heller, M. F. Crommie, C. P. Lutz, and D. M. Eigler, *Nature (London)* **369**, 464 (1994).
- [5] H. C. Manoharan, C. P. Lutz, and D. M. Eigler, *Nature (London)* **403**, 512 (2000).
- [6] C. Rössler, D. Oehri, O. Zilberberg, G. Blatter, M. Karalic, J. Pijnenburg, A. Hofmann, T. Ihn, K. Ensslin, C. Reichl, and W. Wegscheider, *Phys. Rev. Lett.* **115**, 166603 (2015).
- [7] B. Brun, F. Martins, S. Faniel, B. Hackens, A. Cavanna, C. Ulysse, A. Ouerghi, U. Gennser, D. Mailly, P. Simon, S. Huant, V. Bayot, M. Sanquer, and H. Sellier, *Phys. Rev. Lett.* **116**, 136801 (2016).
- [8] D. Goldhaber-Gordon, H. Shtrikman, D. Mahalu, D. Abusch-Magder, U. Meirav, and M. A. Kastner, *Nature (London)* **391**, 156 (1998).
- [9] S. M. Cronenwett, T. H. Oosterkamp, and L. P. Kouwenhoven, *Science* **281**, 540 (1998).
- [10] A. C. Hewson, *The Kondo Problem to Heavy Fermions* (University Press, Cambridge, England, 1997).
- [11] W. B. Thimm, J. Kroha, and J. von Delft, *Phys. Rev. Lett.* **82**, 2143 (1999).
- [12] L. G. G. V. Dias da Silva, N. P. Sandler, K. Ingersent, and S. E. Ulloa, *Phys. Rev. Lett.* **97**, 096603 (2006).
- [13] L. G. G. V. Dias da Silva, K. Ingersent, N. Sandler, and S. Ulloa, *Phys. Rev. B* **78**, 153304 (2008).
- [14] Y. Meir and N. S. Wingreen, *Phys. Rev. Lett.* **68**, 2512 (1992).
- [15] Y. Meir, N. S. Wingreen, and P. A. Lee, *Phys. Rev. Lett.* **70**, 2601 (1993).
- [16] Y. Komijani, R. Yoshii, and I. Affleck, *Phys. Rev. B* **88**, 245104 (2013).
- [17] R. Bulla, T. A. Costi, and T. Pruschke, *Rev. Mod. Phys.* **80**, 395 (2008).
- [18] See Supplemental Material at <http://link.aps.org/supplemental/10.1103/PhysRevLett.119.116801> for additional details, which includes Refs. [19–24].
- [19] M. Abramowitz and I. Stegun, *Handbook of Mathematical Functions: With Formulas, Graphs, and Mathematical Tables*, Applied mathematics series (Dover Publications, New York, 1964).
- [20] W. Hofstetter, *Phys. Rev. Lett.* **85**, 1508 (2000).
- [21] R. Peters, T. Pruschke, and F. B. Anders, *Phys. Rev. B* **74**, 245114 (2006).
- [22] A. Weichselbaum and J. von Delft, *Phys. Rev. Lett.* **99**, 076402 (2007).
- [23] H. Haug and A.-P. Jauho, *Quantum Kinetics in Transport and Optics of Semiconductors* (Springer, New York, 1996).
- [24] D. C. Langreth, *Linear and Nonlinear Electron Transport in Solids*, edited by J. T. Devreese and V. E. van Doren (Plenum Press, New York and London, 1976).
- [25] C. W. Groth, M. Wimmer, A. R. Akhmerov, and X. Waintal, *New J. Phys.* **16**, 063065 (2014).
- [26] The structure studied in Ref. [6] has charging energy $U = 700 \mu\text{eV}$; dot-source (left) and dot-drain (right) coupling $\Gamma_{dL} \approx \Gamma_{dR} \approx 87 \mu\text{eV}$; and cavity mode spacing $\delta_{\text{cav}} \approx 220 \mu\text{eV}$. Using $U = 0.5D \approx 700 \mu\text{eV}$, the NRG scales are then set as $\Gamma_{dL} = \Gamma_{dR} = 0.125U$, and $\delta_{\text{cav}} = 0.32U$. A choice of $\Gamma_{cR} = 0.6D$ yields a conductance peak broadening “ T_{cav} ” $\sim 0.04D = 56 \mu\text{eV}$ in the weak-coupling regime, also consistent with the measured value of $\sim 40 \mu\text{eV}$.
- [27] L. Vaugier, A. A. Aligia, and A. M. Lobos, *Phys. Rev. B* **76**, 165112 (2007).
- [28] L. G. G. V. Dias da Silva, E. Vernek, K. Ingersent, N. Sandler, and S. E. Ulloa, *Phys. Rev. B* **87**, 205313 (2013).
- [29] F. D. M. Haldane, *Phys. Rev. Lett.* **40**, 416 (1978).
- [30] C. Gonzalez-Buxton and K. Ingersent, *Phys. Rev. B* **57**, 14254 (1998).